Computer Aided Geometric Design 44 (2016) 36–55

Contents lists available at ScienceDirect

Computer Aided Geometric Design

www.elsevier.com/locate/cagd

Smooth bivariate shape-preserving cubic spline approximation ☆

Victoria Baramidze

Western Illinois University, 1 University Circle, Macomb, IL 61455, USA

ARTICLE INFO

Article history:
Received 19 October 2015
Received in revised form 4 April 2016
Accepted 25 April 2016
Available online 29 April 2016

Keywords:
Shape preservation
Cubic splines
Bivariate approximation

ABSTRACT

Given a piece-wise linear function defined on a type I uniform triangulation we construct a new partition and define a smooth cubic spline that approximates the linear surface and preserves its shape. The key piece is a new macro-element that has the ability to combine six independent gradients coming together at an interior vertex in a smooth yet shape-preserving fashion. The shape of the resulting spline surface follows local changes in the shape of the piece-wise linear interpolant without overshooting. We prove that convexity, positivity and monotonicity of the spline depend on the local data only. Computational scheme for Bernstein–Bezier spline coefficients is local and fast. Numerical examples highlight unique shape-preserving properties of the spline.

1. Introduction

The concept of shape-preservation rises naturally in data fitting problems. Most often we wish that approximating curves and surfaces preserve positivity, monotonicity and convexity of the data. Various methods have been proposed for constructing shape-preserving spline surfaces. For example, the problem of interpolating scattered positive data is solved by positive splines minimizing a thin-plate energy functional in Utreras (1985). Iterative algorithms are proposed to exploit a variational approach with positivity constraints in Kouibia and Pasadas (2003) and Lai and Meile (2015). Local gradient adjusting methods for non-negative interpolation of scattered data in C^1 macro-element spaces, Powell–Sabin and Clough–Tocher splits, are presented in Schumaker and Speleers (2010). In Carlson and Fritsch (1985) authors develop an algorithm for monotone C^1 piecewise bicubic interpolation on a rectangular mesh. This work is continued in Carlson and Fritsch (1989) by presenting a simplified algorithm producing visually pleasing monotone interpolant. Box splines are studied in Chui et al. (1989), where the estimates for grid-size are obtained to guarantee convexity, monotonicity and positivity of solutions. A degree adaptive method for shape-preserving interpolation over a rectangular grid is presented in Costantini and Fontanella (1990). In Costantini and Manni (1991) the method for construction of differentiable interpolating surfaces over rectangular grids produces co-monotone results. In Schmidt and Hess (1993) interpolation of data sets given on rectangular grids is performed by rational bicubic C^2 splines preserving S-convex, monotone, or positive data. Cubic splines on quadrangulated rectangular grids have been successfully used to define monotone surfaces by requiring linearity of certain cross-boundary derivatives in Schumaker and Han (1997). An extension of Clough–Tocher macro-element allows for a construction of interpolating polynomial splines with surface tension controlled by adaptive polynomial degrees, (Costantini and Manni, 1999). An algorithm for convexity-preserving interpolation of scattered data based on choosing nodal gradients in feasible regions

☆ This paper has been recommended for acceptance by Larry Schumaker.

E-mail address: V-Baramidze@wiu.edu.

http://dx.doi.org/10.1016/j.cagd.2016.04.006
0167-8396/

is presented in Leung and Renka (1999). Cubic L_1 smoothing spline on tensor-product grids in Gilsinn and Lavery (2002) demonstrate promising shape-preserving behavior. An energy functional alternative to the one used in Gilsinn and Lavery (2002) is tested in Witzgall et al. (2006) over Clough–Tocher splits of general irregular triangulations. The ideas of ℓ_1 minimization in Lavery (2001) are adapted for general scattered data triangulations and, compared to thin-plate minimal energy and penalized least squares solutions, experiments demonstrate superior shape-preserving properties of the L_1 splines in Lai and Wenston (2004). Iterative knot insertion algorithm generating a sequence of shape-preserving approximants is given in Kuijt and Damme (2001). In Schumaker and Speleers (2011) a search for a convex spline solution is formulated as a quadratic programming problem where convexity is enforced by including appropriate side conditions on the coefficients of the spline. Rational bi-quadratic splines preserving the shape of 3D positive and convex data are used in Hussain et al. (2011).

Often, researches make global assumptions about the shape of given data, i.e. monotonicity, positivity or convexity, and design algorithms for constructing surfaces preserving the particular feature globally. Many methods are based on a variational approach (Utreras, 1985; Kouibia and Pasadas, 2003; Lai and Meile, 2015; Gilsinn and Lavery, 2002; Lai and Wenston, 2004; Witzgall et al., 2006; Schumaker and Speleers, 2011) resulting either in a large system of equations or an iterative algorithm.

Constructions based on local information and leading to computationally attractive local schemes have been successfully employed as well, see for example (Schumaker and Speleers, 2010; Costantini and Manni, 1991, 1999; Manni, 2001). Macro-element spaces have been extensively used in development of shape-preservation methods, see for example (Willemans and Dierckx, 1994, 1995; Schmidt, 1999; Li, 1999; Lai, 2000; Carnicer et al., 2009).

In this paper we develop a local approach to shape-preservation. In fact, the goal of the construction is to follow local changes in data, and shape-preservation allows us to do so without overshooting.

Let Δ be a triangulation of the domain Ω with function values given at the vertices of Δ. There are some connected subsets of Δ on which the data are positive, and others, where the data are monotone and/or convex. What we claim and prove is that, if on a subset D of Δ the given vertex data is monotone (convex or positive), then for every $0 < \lambda < 1/6$ there exists a set $D_\lambda \subset D$ on which the constructed spline S_λ is monotone (convex or positive), and $\lim_{\lambda\to 0} D_\lambda = D$.

A C^1 cubic spline is a popular choice for many interpolation/approximation problems. Polynomials of relatively low degree are well understood, and many spline tools, such as some macro-elements, for example, are specifically designed for C^1 cubic splines. Spline theory suggests that some of the C^1 conditions across the edges of a type I uniform triangulation are too restrictive, and one will have a problem controlling a cubic spline constructed over Δ due to these restrictions. A single coefficient may affect the spline over the rest of the triangles. There are various macro-element spaces that remedy this problem: after a refinement each coefficient has a finite number of triangles "around" it to control. What we suggest is not, strictly speaking, a refinement of the given Δ, since it does not preserve its edges, nor does it preserve all of its vertices. It is a refinement of Δ in a sense that the new triangulation $\tilde{\Delta}$ consists of many more triangles than Δ, and the geometry and arrangements of these triangles are intimately connected with the original geometry of Δ. A parameter λ controls the size of triangles, and there is more than one $\tilde{\Delta}$ that works (take any $0 < \lambda < 1/6$). This parameter affects the final look of the spline surface, however the surface is shape-preserving for any value of the parameter in the given range.

The constructed spline satisfies many attractive properties and has a few limitations. First of all, a triangulation Δ is not a triangulation of a scattered data set, it is a type I triangulation. Second, the constructed spline interpolates values of a piece-wise linear function, L, at locations other than vertices, while traditionally we seek splines interpolating data at the vertices of Δ. Finally, as an approximation to a piece-wise linear interpolant, the spline produced by the proposed method has regions of flatness, and this feature may limit practical applications of the construction. To minimize regions of flatness larger values of λ must be used. In fact, preliminary testing demonstrates that the case $\lambda = 1/6$ has similar shape-preserving properties. Since $\tilde{\Delta}$ in this case is significantly different, details of this construction and corresponding proofs will have to be reported else-where. Otherwise (if larger λ's are not satisfactory), it is not too difficult to see that ideas presented here can be used in combination with other spline constructions, extended to parametric surfaces, used on parts of domains, etc.

In Section 2 we present detailed construction of $\tilde{\Delta}$. In Section 3 we describe how the coefficients of the spline are computed. We study linearity, positivity, monotonicity, convexity of the spline in Section 4, using results in Lai and Schumaker (2007) to connect the behavior of a BB-polynomial to its coefficients. In Section 5, we discuss numerical experiments performed with shape-preserving splines, and follow up with conclusions in Section 6.

2. Repartitioning a type I uniform triangulation

Let Δ be a type I uniform triangulation of a planar convex domain Ω with the vertices forming a set V, and let $\tilde{\Delta}$ denote the new triangulation. Divide triangles of Δ into two groups, as marked by 1 and 2 in Fig. 1, left (there are two choices for grouping, the key is to alternate triangles from different groups). Fix $0 < \lambda < 1/6$ and associate a weight $w = \lambda$ with triangles marked by 1, and a weight $w = 2\lambda$ with triangles marked by 2. In every triangle $\tau^{(i)} \in \Delta$ with vertices v_1, v_2, v_3 define three points

$$w_1^{(i)} = (1-2w)v_1 + wv_2 + wv_3,$$
$$w_2^{(i)} = wv_1 + (1-2w)v_2 + wv_3,$$

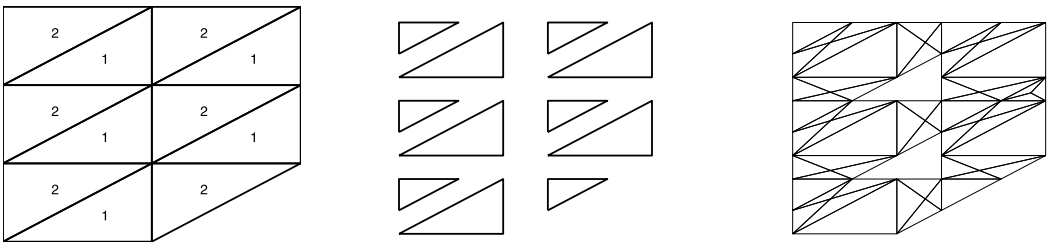

Fig. 1. A given type I uniform triangulation Δ, and steps in defining a suitable repartition $\tilde{\Delta}$.

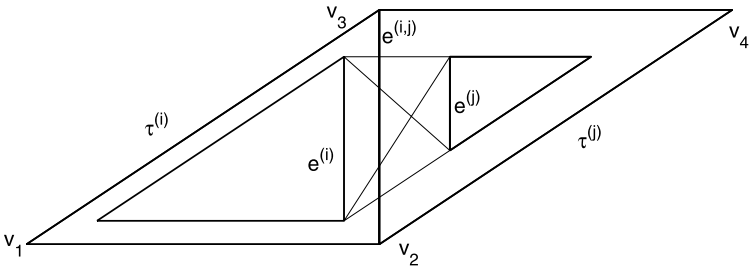

Fig. 2. Creating quadrangles along interior edges.

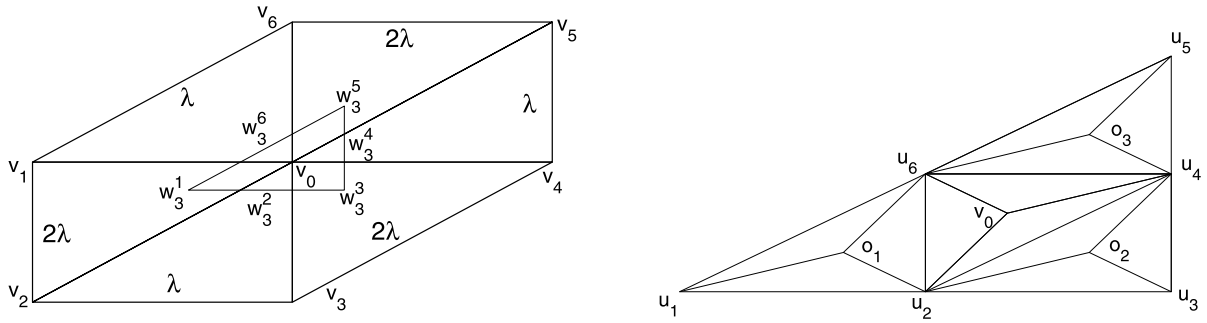

Fig. 3. Left: An interior vertex shared by six triangles leads to the construction of a twelve-triangle macro-element. Right: The twelve-triangle macro-element is made of four CT macro-elements.

$$w_3^{(i)} = wv_1 + wv_2 + (1-2w)v_3, \tag{1}$$

and let W denote the set of all such points in Δ.

Note that $(1-2w, w, w)$ are the barycentric coordinates of $w_1^{(i)}$ with respect to $\tau^{(i)}$. Since they are strictly positive, the point $w_1^{(i)}$ is strictly inside the triangle $\tau^{(i)}$ (similar conclusion holds for the other two points in (1)). The fact that $w_1^{(i)}$ and $w_2^{(i)}$ have identical 3rd barycentric coordinate makes a line segment connecting these two points parallel to the edge opposite to v_3.

Connect the three points in (1) to form a triangle $\tilde{\tau}^{(i)} \subset \tau^{(i)}$ (see Fig. 1, center). The edges of the newly formed triangles are pair-wise parallel to the edges of the original triangles.

For two neighboring triangles $\tau^{(i)}$ and $\tau^{(j)}$ sharing an edge $e^{(i,j)}$ in Δ (see Fig. 2) there are two newly created edges $e^{(i)}$ and $e^{(j)}$ parallel to $e^{(i,j)}$. Connect the four vertices of the two edges to create a quadrangle $\tilde{q}^{(i,j)}$ and its diagonals. Fig. 1, right, demonstrates $\tilde{\Delta}$ after the addition of all quadrangles.

Let v_0 be an interior vertex of the original triangulation Δ. Let $\tau^{(i)} = \langle v_i, v_{i+1}, v_0\rangle$, $i = 1, \ldots, 6$ (identifying v_7 and v_1) be the six triangles sharing v_0 indexed counterclockwise starting with a type 2 triangle, see Fig. 3, left. That is, a parameter w used in computation of $w_j^{(1)}$, $j = 1, 2, 3$ on $\tau^{(1)}$ is equal to 2λ. Consider the polygon formed by the six points $w_3^{(i)} = wv_i + wv_{i+1} + (1-2w)v_0$, $i = 1, \ldots, 6$, with $w = 2\lambda$ for odd i's, and $w = \lambda$ for even i's (see Fig. 3, left). The vertices $w_3^{(i)}$ are ordered counter-clockwise, and it is not to difficult to see that $w_3^{2k} = (w_3^{2k-1} + w_3^{2k+1})/2$, $k = 1, 2, 3$. That is the points $w_3^{2k-1}, w_3^{2k}, w_3^{2k+1}$ are collinear for each $k = 1, 2, 3$, and w_3^{2k} is the midpoint of the line segment $\langle w_3^{2k-1}, w_3^{2k+1}\rangle$. The six vertex polygon is thus reduced to a triangle with vertices $w_3^{(i)}$, $i = 1, 3, 5$.

To simplify the notation we denote $w_3^{(i)}$'s by u_i's (see Fig. 3, right). Define $t_1 = \langle u_6, u_1, u_2\rangle$, $t_2 = \langle u_2, u_3, u_4\rangle$, $t_3 = \langle u_4, u_5, u_6\rangle$ and $t_4 = \langle u_2, u_4, u_6\rangle$. Furthermore, split each of these triangles into three using a barycenter. The barycenter

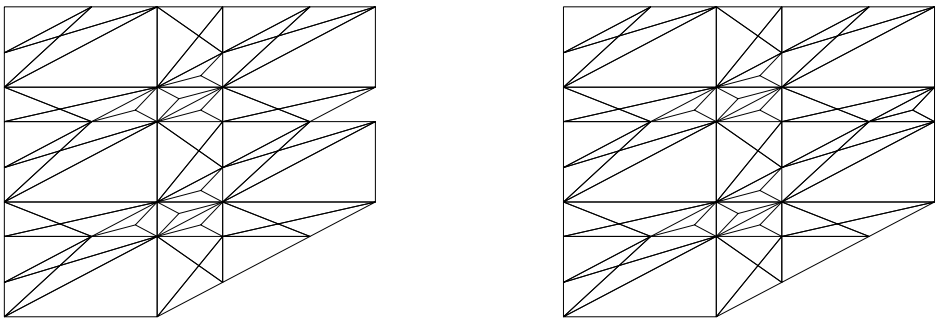

Fig. 4. Last steps is defining $\tilde{\Delta}$.

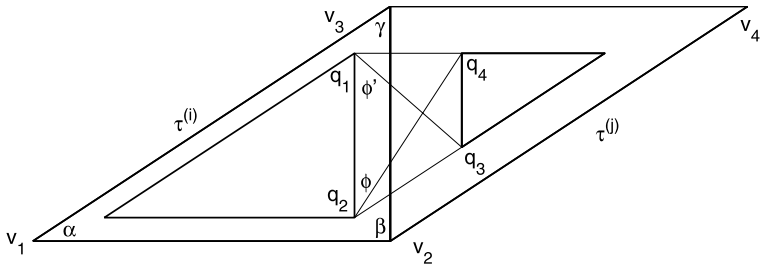

Fig. 5. Angles in a quadrangle.

of t_4 is in fact v_0 (Fig. 3, right). Denote the barycenters of t_i's by o_i's, $i = 1, 2, 3$. Let us call this set of twelve triangles a 12T macro-element. Fig. 4, left, demonstrates how completion of this step affects construction of $\tilde{\Delta}$.

Finally, notice a gap along the right hand side boundary of $\tilde{\Delta}$ in Fig. 4, left. Fill the gaps along the boundary of $\tilde{\Delta}$ by Clough–Tocher macro-triangles (Fig. 4, right). The boundary of $\tilde{\Delta}$ ends up parallel to the boundary of Ω. In fact, define $\tilde{\Omega} = \cup_{t\in\tilde{\Delta}} t$, and note

$$\lim_{\lambda\to 0} W = V,$$
$$\lim_{\lambda\to 0} \tilde{\Delta} = \Delta,$$
$$\lim_{\lambda\to 0} \tilde{\Omega} = \Omega.$$

It will be seen later that for the spline S approximating the piece-wise linear function L

$$\lim_{\lambda\to 0} S = L.$$

Before we proceed with computation of spline coefficients let us comment on the angles in $\tilde{\Delta}$. Note that the four macro-triangles of a 12T macro-element are similar to the triangles in the original triangulation. It is well known that the angles in the split triangles are bounded below, that is the smallest angle in 12T is greater than or equal to a multiple of the smallest angle in Δ (see for example Lemma 4.17 in Lai and Schumaker, 2007). The angles in quadrangles however may be of concern, since they depend on the angles of Δ as well as the value of the parameter λ.

Refer to Fig. 5. Suppose the angles in $\tau^{(i)} = \langle v_1, v_2, v_3\rangle$ have measures α, β and γ at the vertices v_1, v_2 and v_3 respectively. Let q_k, $k = 1, ..., 4$ denote the vertices of the quadrangle, in counterclock order, formed along the edge $\widehat{v_2, v_3}$ with $q_1, q_2 \in \tau^{(i)}$ and $q_3, q_4 \in \tau^{(j)}$. It is easy to recognize that the measure of $\angle q_1, q_2, q_3$ is γ, and the measure of $\angle q_4, q_1, q_2$ is β. The interior angles of $\tilde{q}^{(i,j)}$ at the vertices q_3 and q_4 are $\pi - \gamma$ and $\pi - \beta$ respectively. Let ϕ denote the measure of $\angle q_1, q_2, q_4$, and ϕ' denote the measure of $\angle q_2, q_1, q_3$. Note that the rest of the angles in $\tilde{q}^{(i,j)}$ can be expressed in terms of $\alpha, \beta, \gamma, \phi$ and ϕ'. It not too difficult to check that, if the weight $w = \lambda$ on $\tau^{(i)}$ and it is 2λ on $\tau^{(j)}$, then

$$\cot\phi = \frac{1-3\lambda}{3\lambda}\cot\gamma + \frac{1-6\lambda}{3\lambda}\cot\beta,$$
$$\cot\phi' = \frac{1-3\lambda}{3\lambda}\cot\beta + \frac{1-6\lambda}{3\lambda}\cot\gamma. \tag{2}$$

We see that ϕ and ϕ' decrease as the parameter λ decreases to zero, and the formulas above allow us to choose λ to keep these angles controlled by the angles of the initial triangulation Δ.

3. Computing spline coefficients on $\tilde{\Delta}$

We can formally divide computation of the spline coefficients into three steps according to the three groups of triangulated elements discussed in Section 2.

(i) Define the spline on stand-alone triangles.
(ii) Define the spline on quadrangles.
(iii) Define the spline on 12T macro-elements (Clough–Tocher macro-elements along the boundary are treated similarly to some of the sub-triangles in 12T macro-elements).

3.1. Spline coefficients on a triangle

Let z_k denote the given function value at $v_k \in V$. A linear function defined on $\tau^{(i)} = \langle v_1, v_2, v_3\rangle \in \Delta$ interpolating z_1, z_2, z_3 can be written as

$$L(x, y) = z_1 b_1(x, y) + z_2 b_2(x, y) + z_3 b_3(x, y),$$

where $b_k(x, y)$, $k = 1, 2, 3$ are the barycentric coordinates of a point (x, y) with respect to $\tau^{(i)}$. Evaluate $L(x, y)$ at the locations $w_j^{(i)}$, $j = 1, 2, 3$ defined by (1)

$$\begin{aligned} z_1^{(i)} &:= (1-2w)z_1 + wz_2 + wz_3, \\ z_2^{(i)} &:= wz_1 + (1-2w)z_2 + wz_3, \\ z_3^{(i)} &:= wz_1 + wz_2 + (1-2w)z_3. \end{aligned} \tag{3}$$

The gradient of $L(x, y)$ is constant on $\tau^{(i)}$ and is equal to

$$\nabla L = \sum_{k=1}^{3} z_k \nabla b_k = \frac{1}{2A} \begin{pmatrix} z_1(y_2 - y_3) + z_2(y_3 - y_1) + z_3(y_1 - y_2) \\ z_1(x_3 - x_2) + z_2(x_1 - x_3) + z_3(x_2 - x_1) \end{pmatrix}, \tag{4}$$

with A denoting the area of $\tau^{(i)}$ (in a type I uniform triangulation areas of all triangles are equal). Finally, let us note that directional derivatives of $L(x, y)$ along the edges of $\tau^{(i)}$ are

$$D_{v_k - v_j} L(x, y) = z_k - z_j,\ 1 \le k, j \le 3, k \ne j.$$

For our first step, on every triangle $\tilde{\tau}^{(i)} \subset \tau^{(i)}$ the spline $S(v)$ is linear and interpolates $z_j^{(i)}$ (3) at the vertices $w_j^{(i)}$, $j = 1, 2, 3$ respectively. The Bernstein–Bezier coefficients of this linear piece are

$$c_{jk\ell}^{(i)} = jz_1^{(i)} + kz_2^{(i)} + \ell z_3^{(i)},\ 0 \le j, k, \ell \le 1,\ j + k + \ell = 1.$$

The coefficients of this linear polynomial rewritten as a cubic are

$$C_{jk\ell}^{(i)} = \frac{1}{3}(jz_1^{(i)} + kz_2^{(i)} + \ell z_3^{(i)}),\ 0 \le j, k, \ell \le 3,\ j + k + \ell = 3. \tag{5}$$

3.2. Spline coefficients on a quadrangle

Let $\tilde{q}^{(i,j)}$ denote a quadrangle in $\tilde{\Delta}$ associated with an edge $e^{(i,j)}$ common to the triangles $\tau^{(i)} = \langle v_1, v_2, v_3\rangle$ and $\tau^{(j)} = \langle v_2, v_4, v_3\rangle$ of Δ (Fig. 2). Without loss of generality assume that $\tau^{(i)}$ is from group 1, and $\tau^{(j)}$ is from group 2. Suppose the vertices of $\tilde{q}^{(i,j)}$ are $w_3^{(i)}, w_2^{(i)}, w_1^{(j)}, w_3^{(j)}$ and they are ordered counterclockwise. To simplify the notation we'll denote them by q_i, $i = 1, \ldots, 4$. Suppose the edge $e^{(i,j)}$ intersects the line segments $\langle q_1, q_4\rangle$ and $\langle q_2, q_3\rangle$, at m_1, m_2 respectively. Define the cubic spline $S(v)$ on $\tilde{q}^{(i,j)}$ to satisfy

(i) $S(v)$ interpolates $L(v)$ and its first order derivatives at the vertices of $\tilde{q}^{(i,j)}$,
(ii) $S(v)$ connects smoothly with the spline defined on $\tilde{\tau}^{(i)}$ and $\tilde{\tau}^{(j)}$,
(iii) $S(v)$ interpolates the derivative of $L(v)$ at m_1, m_2 in the direction $e^{(i,j)} = v_3 - v_2$,
(iv) $S(v)$ is C^1 across the interior edges of $\tilde{q}^{(i,j)}$.

Conditions specified above define a unique cubic spline over a quadrilateral macro-element (see Chapter 6.5 in Lai and Schumaker, 2007 for fundamentals on quadrilateral macro-elements).

Define $\mu = \frac{1-6\lambda}{2-9\lambda}$. Then d, the intersection of the diagonals of $\tilde{q}^{(i,j)}$, is

$$d = \mu q_1 + (1-\mu)q_3 = \mu q_2 + (1-\mu)q_4. \tag{6}$$

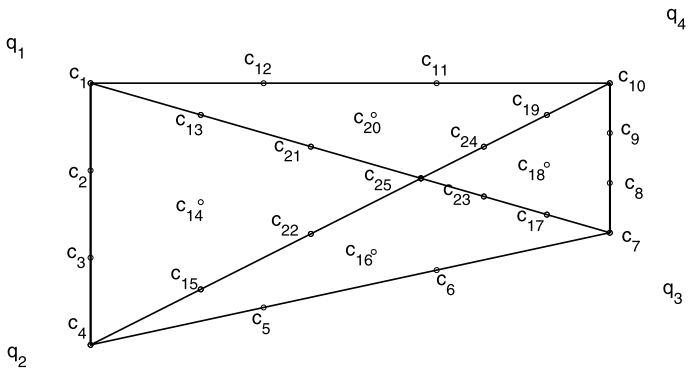

Fig. 6. Domain points over a quadrangle with associated C^0 spline coefficients.

Order the C^0 cubic spline coefficients over $\tilde{q}^{(i,j)}$ as in Fig. 6. Due to linearity of the spline on $\tilde{\tau}^{(i)}$ and continuity of the spline across the edge $\langle q_1, q_2\rangle$ we have

$$\begin{aligned} c_1 &= z_3^{(i)}, \quad c_4 = z_2^{(i)}, \\ c_2 &= \frac{2c_1 + c_4}{3}, \\ c_3 &= \frac{c_1 + 2c_4}{3}. \end{aligned} \tag{7}$$

Due to interpolation of gradients at q_1 and q_2, and smoothness of the spline in the interior of $\tilde{q}^{(i,j)}$ (using (6))

$$\begin{aligned} c_{12} &= c_1 + \lambda(z_2 - z_1), \\ c_{13} &= \mu c_2 + (1-\mu)c_{12}, \\ c_5 &= c_4 + \lambda(z_3 - z_1), \\ c_{15} &= \mu c_3 + (1-\mu)c_5. \end{aligned} \tag{8}$$

Due to linearity of the spline on $\tilde{\tau}^{(i)}$ and C^1 conditions across the edge $\langle q_1, q_2\rangle$ we have

$$c_{14} = \frac{c_{13} + c_{15}}{2}. \tag{9}$$

Similarly

$$\begin{aligned} c_7 &= z_1^{(j)}, \quad c_{10} = z_3^{(j)}, \\ c_8 &= \frac{2c_7 + c_{10}}{3}, \\ c_9 &= \frac{c_7 + 2c_{10}}{3}, \\ c_6 &= c_7 + \lambda(z_2 - z_4), \\ c_{11} &= c_{10} + \lambda(z_3 - z_4), \\ c_{17} &= \mu c_6 + (1-\mu)c_8, \\ c_{19} &= \mu c_{11} + (1-\mu)c_9, \\ c_{18} &= \frac{c_{17} + c_{19}}{2}. \end{aligned} \tag{10}$$

To satisfy conditions (iii), we note that $m_1 = \frac{2q_1+q_4}{3}$ and $m_2 = \frac{2q_2+q_3}{3}$. Since $D_{v_3-v_2}L = z_3 - z_2$ we set

$$D_{v_3-v_2}S(m_1) = D_{v_3-v_2}S(m_2) = z_3 - z_2.$$

Use Lemma 2.11 from Lai and Schumaker (2007) to see that

$$\begin{aligned} D_{v_3-v_2}S(m_1) &= 3(a_1c_{10}+a_2c_{11}+a_3c_{19})\ell_1^2 \\ &\quad + 3(a_1c_{11}+a_2c_{12}+a_3c_{20})2\ell_1\ell_2 \\ &\quad + 3(a_1c_{12}+a_2c_1+a_3c_{13})\ell_2^2, \end{aligned} \tag{11}$$

where $(\ell_1,\ell_2,\ell_3)=(1/3,2/3,0)$ are the barycentric coordinates of m_1 and (a_1,a_2,a_3) are the directional coordinates of v_3-v_2 with respect to $\langle q_4,q_1,d\rangle$. We find that

$$(a_1,a_2,a_3)=\left(\frac{1}{1-6\lambda},\frac{1}{1-3\lambda},-\frac{2-9\lambda}{(1-3\lambda)(1-6\lambda)}\right),$$

and solve (11) for c_{20} to find

$$\begin{aligned} c_{20} &= -\frac{3}{4}\mu(1-3\lambda)(z_3-z_2)+(1-\mu)\lambda(z_3-z_4) \\ &\quad + \mu\lambda(z_2-z_1)+\frac{1-\mu}{12}(13c_{10}-c_7)+\frac{\mu}{3}(4c_1-c_4). \end{aligned} \tag{12}$$

Similarly, since $(2/3,1/3,0)$ are the barycentric coordinates of m_2 in $\langle q_2,q_3,d\rangle$ and

$$(a_1,a_2,a_3)=\left(-\frac{1}{1-3\lambda},-\frac{1}{1-6\lambda},\frac{2-9\lambda}{(1-3\lambda)(1-6\lambda)}\right),$$

are the directional coordinates of v_3-v_2 with respect to $\langle q_2,q_3,d\rangle$, we find that

$$\begin{aligned} c_{16} &= \frac{3}{4}\mu(1-3\lambda)(z_3-z_2)+\mu\lambda(z_3-z_1) \\ &\quad + (1-\mu)\lambda(z_2-z_4)+\frac{1-\mu}{12}(13c_7-c_{10})+\frac{\mu}{3}(4c_4-c_1). \end{aligned} \tag{13}$$

To complete the computation of the coefficients for $\tilde{q}^{(i,j)}$ we set C^1 conditions across the interior edges of $\tilde{q}^{(i,j)}$. Using equation (6)

$$\begin{aligned} c_{21} &= \mu c_{14}+(1-\mu)c_{20}, \\ c_{22} &= \mu c_{14}+(1-\mu)c_{16}, \\ c_{23} &= \mu c_{16}+(1-\mu)c_{18}, \\ c_{24} &= \mu c_{20}+(1-\mu)c_{18}, \\ c_{25} &= \mu c_{21}+(1-\mu)c_{23}. \end{aligned} \tag{14}$$

3.3. Spline coefficients on a 12T macro-element

Coefficients of the spline on a 12T macro-element are computed by following the guidelines below.

(i) Interpolate the values and the gradients of $L(v)$ at each u_i, $i=1,\ldots,6$;
(ii) Interpolate directional derivative of $L(v)$ across the edges $\langle u_i,u_{i+1}\rangle$, $i=1,\ldots,6$ in the directions v_0-v_{i+1};
(iii) Use smoothness conditions to complete 2-sided Clough–Tocher macro-element constructions for the macro-triangles t_1,t_2,t_3;
(iv) Create a traditional Clough–Tocher macro-element spline on t_4 connecting the spline on t_4 to the pieces on t_1, t_2 and t_3 with C^1 continuity.

The $(1,1,0)$-macro element spaces were introduced in Rayevskaya and Schumaker (2005). This construction defines the spline on t_i, $i=1,2,3$. For example, below we show how the conditions above are used on t_2. Organize the coefficients of the spline $c_j^{(2)}$, $j=1,\ldots,19$ on the triangle t_2 as shown in Fig. 7. Then

$$\begin{aligned} c_1^{(2)} &= z_3^{(2)} = \lambda z_2+\lambda z_3+(1-2\lambda)z_0, \\ c_2^{(2)} &= z_3^{(3)} = 2\lambda z_3+2\lambda z_4+(1-4\lambda)z_0, \\ c_3^{(2)} &= z_3^{(4)} = \lambda z_4+\lambda z_5+(1-2\lambda)z_0, \\ c_4^{(2)} &= z_3^{(2)}+(u_3-u_2)\nabla L(u_2)/3 = 2\lambda z_3+(1-2\lambda)z_0, \end{aligned}$$

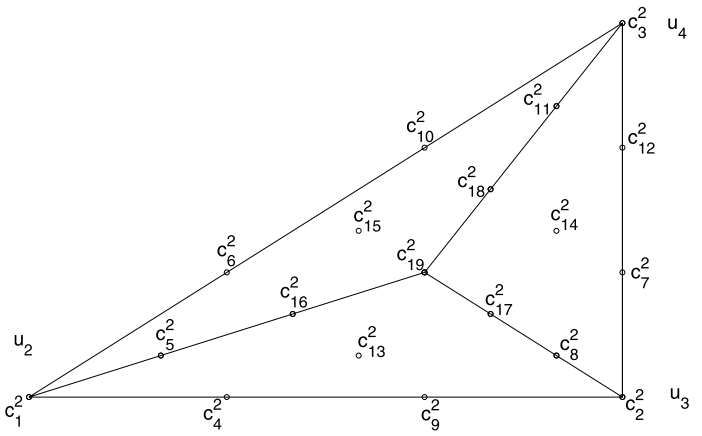

Fig. 7. C^0 domain points and the associated spline coefficients on a CT macro-element.

$$
\begin{aligned}
c_6^{(2)} &= z_3^{(2)} + (u_4 - u_2)\nabla L(u_2)/3 = \lambda z_3 + (1-\lambda) z_0,\\
c_5^{(2)} &= (c_1^{(2)} + c_4^{(2)} + c_6^{(2)})/3,\\
c_7^{(2)} &= z_3^{(3)} + (u_4 - u_3)\nabla L(u_3)/3 = 2\lambda z_4 + \lambda z_3 + (1-3\lambda) z_0,\\
c_9^{(2)} &= z_3^{(3)} + (u_2 - u_3)\nabla L(u_3)/3 = 2\lambda z_3 + \lambda z_4 + (1-3\lambda) z_0,\\
c_8^{(2)} &= (c_2^{(2)} + c_7^{(2)} + c_9^{(2)})/3,\\
c_{10}^{(2)} &= z_3^{(4)} + (u_2 - u_4)\nabla L(u_4)/3 = \lambda z_4 + (1-\lambda) z_0,\\
c_{12}^{(2)} &= z_3^{(4)} + (u_3 - u_4)\nabla L(u_4)/3 = 2\lambda z_4 + (1-2\lambda) z_0,\\
c_{11}^{(2)} &= (c_3^{(2)} + c_{10}^{(2)} + c_{12}^{(2)})/3.
\end{aligned}
\tag{15}
$$

The condition (ii) is applied to the edges $\langle u_2, u_3\rangle$ and $\langle u_3, u_4\rangle$, allowing us to compute the coefficients $c_{13}^{(2)}$ and $c_{14}^{(2)}$. Let m_1 be the point of intersection of $\langle v_0, v_3\rangle$ with $\langle u_2, u_3\rangle$. Let $(a_i)_{i=1}^3$ denote the directional coordinates of $v_0 - v_3$ with respect to $\langle u_2, u_3, o_2\rangle$. It turns out that

$$
(a_1, a_2, a_3) = \left(-\frac{1}{3\lambda}, -\frac{2}{3\lambda}, \frac{1}{\lambda}\right),
$$

and the barycentric coordinates of m_1 with respect to $\langle u_2, u_3, o_2\rangle$ are $(2/3, 1/3, 0)$. Adjusting formula (11) we get

$$
\begin{aligned}
3D_{v_0-v_3}S(m_1) = {} & 4(a_1 c_1^{(2)} + a_2 c_4^{(2)} + a_3 c_5^{(2)})\\
& + 4(a_1 c_4^{(2)} + a_2 c_9^{(2)} + a_3 c_{13}^{(2)})\\
& + (a_1 c_9^{(2)} + a_2 c_2^{(2)} + a_3 c_8^{(2)}).
\end{aligned}
$$

Noting that $D_{v_0-v_3}L(m_1) = z_0 - z_3$ we solve the above equation for $c_{13}^{(2)}$

$$
c_{13}^{(2)} = \frac{\lambda}{3}(5z_3 + 2z_4 - 7z_0) + z_0. \tag{16}
$$

Similarly we find

$$
c_{14}^{(2)} = \frac{\lambda}{3}(2z_3 + 5z_4 - 7z_0) + z_0. \tag{17}
$$

We have no derivative information to interpolate across the edge $\langle u_4, u_2\rangle$. Instead we use the approach in Rayevskaya and Schumaker (2005). That is, we require additional smoothness (C^3) of the spline at the barycenter o_2 across the edge $\langle o_2, u_3\rangle$. Together with the standard C^1 conditions across the interior edges of $\langle u_2, u_3, u_4\rangle$ at o_2 we obtain

$$
c_{15}^{(2)} = \frac{\lambda}{3}(2z_3 + 2z_4 - 4z_0) + z_0, \tag{18}
$$

and

$$
\begin{aligned}
c_{16}^{(2)} &= (c_{13}^{(2)} + c_{15}^{(2)} + c_{5}^{(2)})/3,\\
c_{17}^{(2)} &= (c_{13}^{(2)} + c_{14}^{(2)} + c_{8}^{(2)})/3,\\
c_{18}^{(2)} &= (c_{14}^{(2)} + c_{15}^{(2)} + c_{11}^{(2)})/3,\\
c_{19}^{(2)} &= (c_{16}^{(2)} + c_{17}^{(2)} + c_{18}^{(2)})/3.
\end{aligned} \tag{19}
$$

After determining the coefficients on t_2 and t_3 in an analogous way, we proceed with the coefficients of the spline on t_4. Starting with the obvious and using coefficient indexing similar to the order in Fig. 7

$$
\begin{aligned}
c_{1}^{(4)} &= z_{3}^{(2)} = \lambda z_2 + \lambda z_3 + (1-2\lambda) z_0,\\
c_{2}^{(4)} &= z_{3}^{(4)} = \lambda z_4 + \lambda z_5 + (1-2\lambda) z_0,\\
c_{3}^{(4)} &= z_{3}^{(6)} = \lambda z_6 + \lambda z_1 + (1-2\lambda) z_0,\\
c_{4}^{(4)} &= z_{3}^{(2)} + (u_4 - u_2)\nabla L(u_2)/3 = \lambda z_3 + (1-\lambda) z_0,\\
c_{6}^{(4)} &= z_{3}^{(2)} + (u_6 - u_2)\nabla L(u_2)/3 = \lambda z_2 + (1-\lambda) z_0,\\
c_{7}^{(4)} &= z_{3}^{(4)} + (u_6 - u_4)\nabla L(u_4)/3 = \lambda z_5 + (1-\lambda) z_0,\\
c_{9}^{(4)} &= z_{3}^{(4)} + (u_2 - u_4)\nabla L(u_4)/3 = \lambda z_4 + (1-\lambda) z_0,\\
c_{10}^{(4)} &= z_{3}^{(6)} + (u_2 - u_6)\nabla L(u_6)/3 = \lambda z_1 + (1-\lambda) z_0,\\
c_{12}^{(4)} &= z_{3}^{(6)} + (u_4 - u_6)\nabla L(u_6)/3 = \lambda z_6 + (1-\lambda) z_0,\\
c_{5}^{(4)} &= (c_{1}^{(4)} + c_{4}^{(4)} + c_{6}^{(4)})/3,\\
c_{8}^{(4)} &= (c_{2}^{(4)} + c_{7}^{(4)} + c_{9}^{(4)})/3,\\
c_{11}^{(4)} &= (c_{3}^{(4)} + c_{10}^{(4)} + c_{12}^{(4)})/3.
\end{aligned} \tag{20}
$$

For the coefficient $c_{13}^{(4)}$ note that the barycentric coordinates of v_0 with respect to $\langle u_2, o_2, u_4\rangle$ are $(1,-1,1)$. Using C^1 conditions across the edge $\langle u_2, u_4\rangle$ we find

$$
c_{13}^{(4)} = c_{6}^{(2)} - c_{15}^{(2)} + c_{10}^{(2)} = \frac{\lambda}{3}(z_3 + z_4 - 2z_0) + z_0. \tag{21}
$$

Similarly

$$
c_{14}^{(4)} = \frac{\lambda}{3}(z_5 + z_6 - 2z_0) + z_0, \tag{22}
$$

and

$$
c_{15}^{(4)} = \frac{\lambda}{3}(z_1 + z_2 - 2z_0) + z_0. \tag{23}
$$

The rest of the coefficients are found using formulas similar to (19).

For Clough–Tocher macro-elements along the boundary we use the two-sided approach, similar to how the triangles t_i, $i = 1, 2, 3$ are treated when constructing the spline over a 12T macro-element. The values and gradients of $L(x, y)$ are interpolated at the vertices of the Clough–Tocher macro-elements as well as directional derivatives across the edges neighboring quadrangles. The rest of the coefficients are determined by requiring extra smoothness at the barycenter.

4. Shape of the spline surface

4.1. Convexity

We begin this section by studying the behavior of the spline on a quadrangle. As in Section 3, let $\tau^{(i)} = \langle v_1, v_2, v_3\rangle$ and $\tau^{(j)} = \langle v_2, v_4, v_3\rangle$ be neighboring triangles in Δ, and let $\tilde{q}^{(i,j)}$ be a quadrangle with two edges parallel to $e^{(i,j)} = \langle v_2, v_3\rangle$, the edge in Δ common to $\tau^{(i)}$ and $\tau^{(j)}$.

Proposition 1. *The spline S is linear on $\tilde{q}^{(i,j)}$ in the direction parallel to $e^{(i,j)}$.*

Proof. On the triangle $\langle q_1, q_2, d\rangle$ any line parallel to $e^{(i,j)}$ can be defined as a set of points with the barycentric coordinate $b_3 = K$ for some $0 \le K \le 1$. Then BB-polynomial on this triangle restricted to this line can be described as

$$\begin{aligned} S|_{\langle q_1,q_2,d\rangle}(b_1, b_2, K) &= c_1 b_1^3 + 3c_2 b_1^2 b_2 + 3c_3 b_1 b_2^2 + c_4 b_2^3 \\ &\quad + 3K(c_{13} b_1^2 + 2c_{14} b_1 b_2 + c_{15} b_2^2) \\ &\quad + 3K^2(c_{21} b_1 + c_{22} b_2) + K^3 c_{25}. \end{aligned}$$

Using formulas (7)–(10), (12)–(14) and $b_1 = 1 - b_2 - K$ we get

$$S|_{\langle q_1,q_2,d\rangle}(1 - b_2 - K, b_2, K) = b_2(1 - 3\lambda)(z_2 - z_3) + C(K), \tag{24}$$

where $C(K)$ is a constant independent of b_1 and b_2. Similarly, S is linear on $\langle q_3, q_4, d\rangle$ along any line parallel to $e^{(i,j)}$.

Next, consider $\langle q_4, q_1, d\rangle$. If the barycentric coordinates of a point v restricted to a line parallel to $e^{(i,j)}$ with respect to $\langle q_1, q_2, d\rangle$ are (b_1, b_2, K), then the barycentric coordinates of v with respect to $\langle q_4, q_1, d\rangle$ are

$$(b_1, K + \frac{b_2}{\mu}, -\frac{b_2(1-\mu)}{\mu}).$$

Then the spline on $\langle q_4, q_1, d\rangle$ restricted to a line parallel to $e^{(i,j)}$ can be simplified using $b_1 = 1 - b_2 - K$ as

$$S|_{\langle q_4,q_1,d\rangle}(1 - b_2 - K, K + \frac{b_2}{\mu}, -\frac{b_2(1-\mu)}{\mu}) = b_2(1 - 3\lambda)(z_2 - z_3) + C(K),$$

where the constant $C(K)$ is identical to the one in (24).

The following results are concerned with convexity of the spline.

Let $L^{(i)}(v)$ denote the restriction of $L(v)$ to $\tau^{(i)}$. Note that if $z_4 > (<) L^{(i)}(v_4)$ then $L(v)$ is concave up (down) on $\tau^{(i)} \cup \tau^{(j)}$. If $z_4 = L^{(i)}(v_4)$ then the points (v_k, z_k), $k = 1, 2, 3, 4$ are coplanar. □

Theorem 1. *The spline S restricted to $\tilde{q}^{(i,j)}$ preserves concavity of $L(v)$ on $\tau^{(i)} \cup \tau^{(j)}$.*

Proof. We will show that the result holds on the sub-triangles $\langle q_1, q_2, d\rangle$ and $\langle q_4, q_1, d\rangle$. Since our construction is symmetric the result follows for the other two sub-triangles of $\tilde{q}^{(i,j)}$.

According to Theorem 3.15 of Lai and Schumaker (2007) we need to consider the matrices A_{ijk}, $i + j + k = 1$ which on $\langle q_1, q_2, d\rangle$ simplify as

$$\begin{aligned} A_{100} &= \lambda(1-\mu)^2(z_4 - L^{(i)}(v_4)) \begin{bmatrix} 0 & 0 \\ 0 & 1 \end{bmatrix}, \\ A_{010} &= \lambda(1-\mu)^2(z_4 - L^{(i)}(v_4)) \begin{bmatrix} 0 & 0 \\ 0 & 1 \end{bmatrix}, \\ A_{001} &= \mu\lambda(1-\mu)^2(z_4 - L^{(i)}(v_4)) \begin{bmatrix} 0 & 0 \\ 0 & 1 \end{bmatrix}. \end{aligned}$$

Here $(1-\mu)^2$, λ, and μ are positive (as long as we keep $1 - 6\lambda$ positive), while the sign of the difference $z_4 - L^{(i)}(v_4)$ depends on the concavity of $L(v)$ on $\tau^{(i)} \cup \tau^{(j)}$. Similarly,

$$\begin{aligned} A_{100} &= \begin{bmatrix} 0 & 0 \\ 0 & 0 \end{bmatrix}, \\ A_{010} &= \lambda(z_4 - L^{(i)}(v_4)) \begin{bmatrix} 1 & \mu \\ \mu & \mu^2 \end{bmatrix}, \\ A_{001} &= \mu\lambda(z_4 - L^{(i)}(v_4)) \begin{bmatrix} 1 & \mu \\ \mu & \mu^2 \end{bmatrix}, \end{aligned}$$

imply preservation of concavity of $L(v)$ on $\langle q_4, q_1, d\rangle$. □

Let t_2 be a triangle with vertices u_2, u_3, u_4 and a barycenter o_2 as in Section 3.2. Additionally let $\delta_i = z_i - z_{i+1} + z_{i+2} - z_0$, and note that $\delta_i = z_{i+2} - L^{(i)}(v_{i+2}) > 0$ implies $L(v)$ is concave up on $\tau^{(i)} \cup \tau^{(i+1)}$.

Theorem 2. *Suppose $L(v)$ is concave up on $\tau^{(2)} \cup \tau^{(3)} \cup \tau^{(4)}$. The spline S restricted to t_2 is concave up as well.*

Proof. Consider the triangle $\langle u_2, u_3, o_2\rangle$ and the matrices

$$A_{100} = \frac{\lambda}{9}\delta_2 \begin{bmatrix} 9 & 6 \\ 6 & 4 \end{bmatrix},$$
$$A_{010} = \begin{bmatrix} 0 & 0 \\ 0 & 0 \end{bmatrix},$$
$$A_{001} = \frac{\lambda}{27}\delta_2 \begin{bmatrix} 9 & 6 \\ 6 & 4 \end{bmatrix} + \frac{\lambda}{27}\delta_3 \begin{bmatrix} 0 & 0 \\ 0 & 1 \end{bmatrix}. \tag{25}$$

The linear function $L(v)$ is concave up on $\tau^{(2)} \cup \tau^{(3)} \cup \tau^{(4)}$ if both $\delta_2 > 0$ and $\delta_3 > 0$, or if one quantity is strictly positive, while the other is zero. By Theorem 3.15 in Lai and Schumaker (2007), if $\delta_2 > 0$ and $\delta_3 > 0$, the spline is concave up on $\langle u_2, u_3, o_2\rangle$. If one of the quantities is zero, the spline's concavity depends on the sign of the other. If $\delta_2 = \delta_3 = 0$, that is the points (v_i, z_i), $i = 2, 3, 4, 5$ and (v_0, z_0) are coplanar, the spline is linear on $\langle u_2, u_3, o_2\rangle$. Due to symmetry of our construction we skip similar considerations for $\langle u_3, u_4, o_2\rangle$, and move on to studying the behavior of S on $\langle u_4, u_2, o_2\rangle$.

We find that the matrices of interest are

$$A_{100} = \frac{\lambda}{9}\delta_3 \begin{bmatrix} 9 & 6 \\ 6 & 4 \end{bmatrix},$$
$$A_{010} = \frac{\lambda}{9}\delta_2 \begin{bmatrix} 9 & 3 \\ 3 & 1 \end{bmatrix},$$
$$A_{001} = \frac{\lambda}{27}\delta_2 \begin{bmatrix} 9 & 3 \\ 3 & 1 \end{bmatrix} + \frac{\lambda}{27}\delta_3 \begin{bmatrix} 9 & 6 \\ 6 & 4 \end{bmatrix},$$

and all claimed conclusions follow again. □

Due to symmetry of the construction, the behavior of S on t_1 and t_3 is similar to that of S on t_2. It remains to show, however, that

Theorem 3. *If $L(v)$ on $\cup_{i=1}^{6}\tau^{(i)}$ is concave up, then the spline S restricted to t_4 is concave up as well.*

Proof. It suffices to show that the result holds on one of the micro-triangles of t_4. For example, consider $\langle u_2, u_4, v_0\rangle$ and the matrices

$$A_{100} = \frac{\lambda}{9}\delta_2 \begin{bmatrix} 9 & 3 \\ 3 & 1 \end{bmatrix} + \frac{\lambda}{9}\delta_1 \begin{bmatrix} 0 & 0 \\ 0 & 1 \end{bmatrix},$$
$$A_{010} = \frac{\lambda}{9}\delta_3 \begin{bmatrix} 9 & 6 \\ 6 & 4 \end{bmatrix} + \frac{\lambda}{9}\delta_4 \begin{bmatrix} 0 & 0 \\ 0 & 1 \end{bmatrix},$$
$$A_{001} = \frac{\lambda}{27}(\delta_2 + \delta_5) \begin{bmatrix} 9 & 3 \\ 3 & 1 \end{bmatrix} + \frac{\lambda}{27}(\delta_3 + \delta_6) \begin{bmatrix} 9 & 6 \\ 6 & 4 \end{bmatrix}$$
$$+ \frac{\lambda}{27}(\delta_3 - \delta_6 + 2\delta_4) \begin{bmatrix} 0 & 0 \\ 0 & 1 \end{bmatrix}.$$

Clearly, A_{ijk}, $i+j+k=1$ are non-negative definite if $\delta_i \geq 0$, $i = 1, \ldots, 6$ and $\delta_3 - \delta_6 + 2\delta_4 \geq 0$. The last inequality is equivalent to

$$z_2 + z_5 \leq z_3 + z_4 + z_6 + z_1 - 2z_0. \tag{26}$$

Since δ_1 and δ_2 are nonnegative $z_2 \leq z_1 + z_3 - z_0$ and $z_5 \leq z_4 + z_6 - z_0$, and therefore (26) follows. □

To sum up, if $L(v)$ is concave up (down) on $\cup_{i=1}^{6}\tau^{(i)}$, then $\delta_i \geq (\leq) 0$, $i = 1, \ldots, 6$. By Theorem 3.15 in Lai and Schumaker (2007) and Theorems 1, 2 above the spline S is concave up (down) on t_i, $i = 1, \ldots, 4$, and on each of the six quadrangles along the edges $\langle v_0, v_i\rangle$, $i = 1, \ldots, 6$ of the original triangulation.

If the concavity of $L(v)$ around v_0 changes, that is the data inflects, then δ_i's have different signs and the spline inflects. It is interesting to see how the spline changes along the three edge directions of the original triangulation.

Theorem 4. *Suppose $\delta_2 > 0$ and $\delta_3 < 0$. On the triangle $\langle u_2, u_3, o_2\rangle$ the spline is*

(i) *concave up in the direction $u_3 - u_2$,*
(ii) *concave down in the direction $u_4 - u_3$,*

(iii) *concave up in the direction $u_4 - u_2$ if in addition $|\delta_3| < |\delta_2|$.*

Proof. In the triangle $\langle u_2, u_3, o_2\rangle$ by Theorem 3.14 (Lai and Schumaker, 2007), and using the matrices (25), for the direction $u = u_3 - u_2 = 1(u_3 - u_2) + 0(o_2 - u_2)$ the expressions

$$(1\ 0)A_{ijk}(1\ 0)^T$$

depend on δ_2 only. Indeed

$$\begin{aligned}
(1\ 0)A_{100}(1\ 0)^T &= \lambda\delta_2,\\
(1\ 0)A_{010}(1\ 0)^T &= 0,\\
(1\ 0)A_{001}(1\ 0)^T &= \frac{\lambda}{3}\delta_2.
\end{aligned}$$

Since δ_2 is positive the spline restricted to a line parallel to $u_3 - u_2$ is concave up.

The direction $u_4 - u_3$ can be expressed as $3(o_2 - u_2) - 2(u_3 - u_2)$, then

$$\begin{aligned}
(-2\ 3)A_{100}(-2\ 3)^T &= 0,\\
(-2\ 3)A_{010}(-2\ 3)^T &= 0,\\
(-2\ 3)A_{001}(-2\ 3)^T &= \frac{\lambda}{3}\delta_3.
\end{aligned}$$

Clearly, the spline is concave down in the direction $u_4 - u_3$.

Finally, the direction $u_4 - u_2$ can be expressed as $3(o_2 - u_2) - 1(u_3 - u_2)$, and thus we consider the expressions

$$\begin{aligned}
(-1\ 3)A_{100}(-1\ 3)^T &= \lambda\delta_2,\\
(-1\ 3)A_{010}(-1\ 3)^T &= 0,\\
(-1\ 3)A_{001}(-1\ 3)^T &= \frac{\lambda}{3}(\delta_2 + \delta_3).
\end{aligned}$$

Clearly, in the direction $u_4 - u_2$ the spline is concave up as long as $|\delta_3| < |\delta_2|$. □

Theorem 5. *Suppose $sign(\delta_2) = -sign(\delta_3)$. The spline restricted to the triangle $\langle u_4, u_2, o_2\rangle$ inflects along every line $b_3 = k$, $0 \le k \le 1$, parallel to the edge $\langle u_4, u_2\rangle$. The inflection point lies inside the triangle for every $k < \min\left\{\frac{3\delta_3}{2\delta_3-\delta_2}, \frac{3\delta_2}{2\delta_2-\delta_3}\right\} =: M$.*

Proof. A line parallel to the edge $\langle u_4, u_2\rangle$ and crossing the interior of $\langle u_4, u_2, o_2\rangle$ can be defined as

$$\ell(t) = u_4(1-t) + u_2(t-k) + o_2k,$$

for $0 \le k \le 1$. The line segment inside the triangle corresponds to values of t between k and 1. The spline along this line has a second order derivative

$$2\lambda(3\delta_3 + 3t(\delta_2 - \delta_3) + k(-2\delta_2 + \delta_3)),$$

and an inflection point

$$t_{inf} = \frac{-3\delta_3 + (2\delta_2 - \delta_3)k}{3(\delta_2 - \delta_3)}.$$

Case 1: Suppose $\delta_2 > 0$ and $\delta_3 < 0$. Then the condition $k < t_{inf}$ is equivalent to

$$k < \frac{3\delta_3}{2\delta_3 - \delta_2}.$$

The condition $t_{inf} < 1$ is equivalent to

$$k < \frac{3\delta_2}{2\delta_2 - \delta_3}.$$

Thus $k < t_{inf} < 1$ as long as

$$k < M.$$

Case 2: Suppose $\delta_2 < 0$ and $\delta_3 > 0$. Then the condition $k < t_{inf}$ is equivalent to

$$k < \frac{3\delta_3}{2\delta_3 - \delta_2}.$$

The condition $t_{inf} < 1$ is equivalent to

$$k < \frac{3\delta_2}{2\delta_2 - \delta_3}.$$

Since $M \le 1$, the point t_{inf} is inside the triangle when $k \le M$. If $M < 1$, the inflection point vanishes from the triangle as soon as k exceeds M. □

Theorem 6. *Suppose* $sign(\delta_2) = -sign(\delta_3)$. *The spline restricted to the triangle* $\langle u_2, u_4, v_0\rangle$ *inflects along every line* $b_3 = k$, $0 \le k \le 1$, *parallel to the edge* $\langle u_2, u_4\rangle$. *The inflection point is inside the triangle for every* $k < \min\left\{\frac{3\delta_3}{\delta_3 - 2\delta_2}, \frac{3\delta_2}{\delta_2 - 2\delta_3}\right\} =: M'$.

Proof. A line parallel to the edge $\langle u_2, u_4\rangle$ and crossing the interior of $\langle u_2, u_4, v_0\rangle$ can be defined as

$$\ell(t) = u_2(1-t) + u_4(t-k) + v_0 k,$$

for $0 \le k \le 1$. The spline restricted to this line and differentiated twice (with respect to t) is defined by

$$2\lambda(-\delta_3(k-3t) + \delta_2(3+2k-3t)),$$

and its only inflection point is

$$t_{inf} = \frac{3\delta_2 + (2\delta_2 - \delta_3)k}{3(\delta_2 - \delta_3)}.$$

This point is interior to the triangle when $k \le M'$, since $M' \le 1$. If $M' < 1$, the inflection point vanishes from the triangle as soon as k exceeds M'. □

4.2. Monotonicity

Let us now study monotonicity of the spline on a quadrangle $\tilde{q}^{(i,j)}$, constructed along the edge $\langle v_2, v_3\rangle$, common to triangles $\tau^{(i)} = \langle v_1, v_2, v_3\rangle$ and $\tau^{(j)} = \langle v_2, v_4, v_3\rangle$.

Theorem 7. *The spline restricted to* $\tilde{q}^{(i,j)}$ *preserves monotonicity of* $L(v)$ *on* $\tau^{(i)} \cup \tau^{(j)}$.

Proof. Let q_k, $k = 1, \ldots, 4$ denote the vertices of $\tilde{q}^{(i,j)} = \langle w_3^{(i)}, w_2^{(i)}, w_1^{(j)}, w_3^{(j)}\rangle$. The directions $q_2 - q_1, q_3 - q_2, q_4 - q_1$ are the same as the directions of $v_2 - v_3, v_4 - v_2 = v_3 - v_1, v_2 - v_1 = v_4 - v_3$. Consider the spline behavior along these directions. According to Theorem 3.10 in Lai and Schumaker (2007), a cubic BB-polynomial is monotone increasing on a triangle t in a direction u if

$$a_1 c_{i+1,j,k} + a_2 c_{i,j+1,k} + a_3 c_{i,j,k+1} \ge 0, \; i + j + k = 2. \tag{27}$$

Here (a_1, a_2, a_3) are the directional coordinates of u with respect to the triangle t.

First consider the triangle $\langle q_1, q_2, d\rangle$. In the direction $v_2 - v_3$ we have $(-1, 1, 0)$ as the directional coordinates in question, and thus expressions in (27) are

$$c_4 - c_3 = c_3 - c_2 = c_2 - c_1 = c_{15} - c_{14} = c_{14} - c_{13} = c_{22} - c_{21} = (1 - 3w)(z_2 - z_3)/3.$$

The quantity $(1 - 3w)$ is positive for $0 < \lambda < 1/6$, the value $z_2 - z_1$ is positive if $L(v)$ is increasing from v_3 towards v_2. By Theorem 3.10 in Lai and Schumaker (2007) the spline preserves monotonicity of the data in the direction $v_2 - v_3$. Next, let a denote the triple of directional coordinates of $q_3 - q_2$ with respect to $\langle q_1, q_2, d\rangle$. We find that

$$a = \left(-\frac{\mu}{1-\mu}, -1, \frac{1}{1-\mu}\right),$$

and expressions in (27) become

$$-\frac{\mu}{1-\mu}c_1 - c_2 + \frac{1}{1-\mu}c_{13} = \lambda(z_3 - z_1),$$
$$-\frac{\mu}{1-\mu}c_2 - c_3 + \frac{1}{1-\mu}c_{14} = \lambda(z_3 - z_1),$$
$$-\frac{\mu}{1-\mu}c_3 - c_4 + \frac{1}{1-\mu}c_{15} = \lambda(z_3 - z_1),$$

$$-\frac{\mu}{1-\mu}c_{13}-c_{14}+\frac{1}{1-\mu}c_{21}=\lambda(\mu(z_3-z_1)+(1-\mu)(z_4-z_2)),$$
$$-\frac{\mu}{1-\mu}c_{14}-c_{15}+\frac{1}{1-\mu}c_{22}=\lambda(\mu(z_3-z_1)+(1-\mu)(z_4-z_2)),$$
$$-\frac{\mu}{1-\mu}c_{21}-c_{22}+\frac{1}{1-\mu}c_{25}=\lambda(\mu^2(z_3-z_1)+(1-\mu^2)(z_4-z_2)).$$

The spline is monotone increasing in the direction q_3-q_2 if $L(v)$ increases from v_1 towards v_3 and from v_2 towards v_4. Since the directions q_3-q_2, v_3-v_1 and v_4-v_2 are the same, the spline preserves monotonicity of $L(v)$ in the direction q_3-q_2. Now, let a denote the triple of directional coordinates of q_4-q_1 with respect to $\langle q_1,q_2,d\rangle$. We find that

$$a=\left(-1,-\frac{\mu}{1-\mu},\frac{1}{1-\mu}\right),$$

and

$$-c_1-\frac{\mu}{1-\mu}c_2+\frac{1}{1-\mu}c_{13}=\lambda(z_2-z_1),$$
$$-c_2-\frac{\mu}{1-\mu}c_3+\frac{1}{1-\mu}c_{14}=\lambda(z_2-z_1),$$
$$-c_3-\frac{\mu}{1-\mu}c_4+\frac{1}{1-\mu}c_{15}=\lambda(z_2-z_1),$$
$$-c_{13}-\frac{\mu}{1-\mu}c_{14}+\frac{1}{1-\mu}c_{21}=\lambda(\mu(z_2-z_1)+(1-\mu)(z_4-z_3)),$$
$$-c_{14}-\frac{\mu}{1-\mu}c_{15}+\frac{1}{1-\mu}c_{22}=\lambda(\mu(z_2-z_1)+(1-\mu)(z_4-z_3)),$$
$$-c_{21}-\frac{\mu}{1-\mu}c_{22}+\frac{1}{1-\mu}c_{25}=\lambda(\mu^2(z_2-z_1)+(1-\mu^2)(z_4-z_3)).$$

The spline is monotone increasing in the direction q_4-q_1 if $L(v)$ increases from v_1 towards v_2 and from v_3 towards v_4. Since the directions q_4-q_1, v_2-v_1 and v_4-v_3 are the same, the spline preserves monotonicity of $L(v)$.

Now consider the triangle $\langle q_2,q_3,d\rangle$. Directional coordinates of q_2-q_1 are $(-1,-\frac{1-\mu}{\mu},\frac{1}{\mu})$, and

$$-c_4-\frac{1-\mu}{\mu}c_5+\frac{1}{\mu}c_{15}=(1-3w)(z_2-z_3)/3$$
$$-c_5-\frac{1-\mu}{\mu}c_6+\frac{1}{\mu}c_{16}=(1-3w)(z_2-z_3)/3,$$
$$-c_6-\frac{1-\mu}{\mu}c_7+\frac{1}{\mu}c_{17}=(1-3w)(z_2-z_3)/3,$$
$$-c_{15}-\frac{1-\mu}{\mu}c_{16}+\frac{1}{\mu}c_{22}=(1-3w)(z_2-z_3)/3,$$
$$-c_{16}-\frac{1-\mu}{\mu}c_{17}+\frac{1}{\mu}c_{23}=(1-3w)(z_2-z_3)/3,$$
$$-c_{22}-\frac{1-\mu}{\mu}c_{23}+\frac{1}{\mu}c_{25}=(1-3w)(z_2-z_3)/3.$$

Theorem 3.10 in Lai and Schumaker (2007) implies that in this triangle in the direction v_2-v_3 the spline preserves monotonicity of the data. Similarly, we find that $(-1,1,0)$ are the directional coordinates of q_3-q_2 with respect to $\langle q_2,q_3,d\rangle$. Then

$$c_5-c_4=\lambda(z_3-z_1),$$
$$c_6-c_5=\lambda(z_4-z_2),$$
$$c_7-c_6=\lambda(z_4-z_2),$$
$$c_{16}-c_{15}=\lambda(\mu(z_3-z_1)+(1-\mu)(z_4-z_2)),$$
$$c_{17}-c_{16}=\lambda(z_4-z_2),$$
$$c_{23}-c_{22}=\lambda(\mu^2(z_3-z_1)+(1-\mu^2)(z_4-z_2)),$$

and conclusions follow. Finally, the triple of directional coordinates of $q_4 - q_1$ with respect to $\langle q_2, q_3, d\rangle$ are

$$a = \left(-\frac{\mu}{1-\mu}, \frac{1-\mu}{\mu}, \frac{2\mu-1}{\mu(1-\mu)}\right).$$

Then

$$\begin{aligned}
&-\frac{\mu}{1-\mu}c_4 + \frac{1-\mu}{\mu}c_5 + \frac{2\mu-1}{\mu(1-\mu)}c_{15} = (1-3w)(z_2-z_1)/3,\\
&-\frac{\mu}{1-\mu}c_5 + \frac{1-\mu}{\mu}c_6 + \frac{2\mu-1}{\mu(1-\mu)}c_{16} = (1-3w)(z_4-z_3)/3,\\
&-\frac{\mu}{1-\mu}c_6 + \frac{1-\mu}{\mu}c_7 + \frac{2\mu-1}{\mu(1-\mu)}c_{17} = (1-3w)(z_4-z_3)/3,\\
&-\frac{\mu}{1-\mu}c_{15} + \frac{1-\mu}{\mu}c_{16} + \frac{2\mu-1}{\mu(1-\mu)}c_{22} = \lambda(\mu(z_2-z_1) + (1-\mu)(z_4-z_3)),\\
&-\frac{\mu}{1-\mu}c_{16} + \frac{1-\mu}{\mu}c_{17} + \frac{2\mu-1}{\mu(1-\mu)}c_{23} = (1-3w)(z_4-z_3)/3,\\
&-\frac{\mu}{1-\mu}c_{22} + \frac{1-\mu}{\mu}c_{23} + \frac{2\mu-1}{\mu(1-\mu)}c_{25} = \lambda(\mu^2(z_2-z_1) + (1-\mu^2)(z_4-z_3)),
\end{aligned}$$

and we reach similar conclusions. Due to the symmetry of our construction we do not have to consider the triangles $\langle q_3, q_4, d\rangle$ and $\langle q_4, q_1, d\rangle$. □

Monotonicity of the spline on a 12T macro-element with a central vertex v_0 depends on the behavior of $L(v)$ on the six triangles having v_0 in common. Refer to Sections 2 and 3 for the notation and geometry. We restrict our attention to macro-triangles $\langle u_2, u_3, u_4\rangle$, barycenter o_2, and $\langle u_2, u_4, u_6\rangle$, barycenter v_0.

Theorem 8. *The spline restricted to the 12T macro-element around a vertex v_0 preserves monotonicity of $L(v)$ on $\cup_{i=1}^{6}\tau^{(i)}$.*

Proof. First consider expressions $a_1c_{i+1,j,k} + a_2c_{i,j+1,k} + a_3c_{i,j,k+1}$ on $\langle u_2, u_3, o_2\rangle$ in the direction $u_3 - u_2$ (this direction is the same as the directions $v_3 - v_2$, $v_5 - v_6$, $v_4 - v_0$, $v_0 - v_1$). Directional coordinates (a_1, a_2, a_3) of $u_3 - u_2$ are $(-1, 1, 0)$, and

$$\begin{aligned}
&-c_1^{(2)} + c_4^{(2)} = \lambda(z_3 - z_2),\\
&-c_4^{(2)} + c_9^{(2)} = \lambda(z_4 - z_0),\\
&-c_9^{(2)} + c_2^{(2)} = \lambda(z_4 - z_0),\\
&-c_5^{(2)} + c_{13}^{(2)} = \lambda/3(z_3 - z_2) + 2\lambda/3(z_4 - z_0),\\
&-c_{13}^{(2)} + c_8^{(2)} = \lambda(z_4 - z_0),\\
&-c_{16}^{(2)} + c_{17}^{(2)} = \lambda/9(z_3 - z_2) + 8\lambda/9(z_4 - z_0),
\end{aligned}$$

imply that the spline monotonicity is controlled by the behavior of $L(v)$ along the edges $\langle v_3, v_2\rangle$ and $\langle v_4, v_0\rangle$. For the direction $u_4 - u_3$ (this direction is the same as the directions $v_5 - v_4$, $v_6 - v_0$, $v_1 - v_2$, $v_0 - v_3$), directional coordinates are $(-1, -2, 3)$, and

$$\begin{aligned}
&-c_1^{(2)} - 2c_4^{(2)} + 3c_5^{(2)} = \lambda(z_0 - z_3),\\
&-c_4^{(2)} - 2c_9^{(2)} + 3c_{13}^{(2)} = \lambda(z_0 - z_3),\\
&-c_9^{(2)} - 2c_2^{(2)} + 3c_8^{(2)} = \lambda(z_0 - z_3),\\
&-c_5^{(2)} - 2c_{13}^{(2)} + 3c_{16}^{(2)} = \lambda(z_0 - z_3),\\
&-c_{13}^{(2)} - 2c_8^{(2)} + 3c_{17}^{(2)} = \lambda(z_0 - z_3),\\
&-c_{16}^{(2)} - 2c_{17}^{(2)} + 3c_{19}^{(2)} = \lambda/9(z_5 - z_4) + 8\lambda/9(z_0 - z_3),
\end{aligned}$$

imply that the spline monotonicity is controlled by the behavior of $L(v)$ along the edges $\langle v_3, v_0\rangle$ and $\langle v_4, v_5\rangle$. For the direction $u_4 - u_2$ (this direction is the same as the directions $v_5 - v_0$, $v_0 - v_2$, $v_6 - v_1$, $v_4 - v_3$), directional coordinates are $(-2, -1, 3)$, and

$$
\begin{aligned}
&-2c_1^{(2)} - c_4^{(2)} + 3c_5^{(2)} = \lambda(z_0 - z_2),\\
&-2c_4^{(2)} - c_9^{(2)} + 3c_{13}^{(2)} = \lambda(z_4 - z_3),\\
&-2c_9^{(2)} - c_2^{(2)} + 3c_8^{(2)} = \lambda(z_4 - z_3),\\
&-2c_5^{(2)} - c_{13}^{(2)} + 3c_{16}^{(2)} = \lambda/3(z_0 - z_2) + 2\lambda/3(z_4 - z_3),\\
&-2c_{13}^{(2)} - c_8^{(2)} + 3c_{17}^{(2)} = \lambda(z_4 - z_3),\\
&-2c_{16}^{(2)} - c_{17}^{(2)} + 3c_{19}^{(2)} = \lambda/9(z_5 - z_0) + \lambda/9(z_0 - z_2) + 7\lambda/9(z_4 - z_3),
\end{aligned}
$$

imply that the spline's monotonicity is controlled by the behavior of $L(v)$ along the edges $\langle v_4, v_3\rangle$, $\langle v_5, v_0\rangle$ and $\langle v_0, v_2\rangle$.

Consider the triangle $\langle u_4, u_2, o_2\rangle$ next. Along the same 3 directions, we get

$$
\begin{aligned}
&-c_3^{(2)} - 2c_{10}^{(2)} + 3c_{11}^{(2)} = \lambda(z_4 - z_0),\\
&-c_{10}^{(2)} - 2c_6^{(2)} + 3c_{15}^{(2)} = \lambda(z_4 - z_0),\\
&-c_6^{(2)} - 2c_1^{(2)} + 3c_5^{(2)} = \lambda(z_3 - z_2),\\
&-c_{11}^{(2)} - 2c_{15}^{(2)} + 3c_{18}^{(2)} = \lambda(z_4 - z_0),\\
&-c_{15}^{(2)} - 2c_5^{(2)} + 3c_{16}^{(2)} = \lambda/3(z_3 - z_2) + 2\lambda/3(z_4 - z_0),\\
&-c_{18}^{(2)} - 2c_{16}^{(2)} + 3c_{19}^{(2)} = \lambda/9(z_3 - z_2) + 8\lambda/9(z_4 - z_0),
\end{aligned}
$$

in the direction $u_3 - u_2$,

$$
\begin{aligned}
&2c_3^{(2)} + c_{10}^{(2)} - 3c_{11}^{(2)} = \lambda(z_5 - z_4),\\
&2c_{10}^{(2)} + c_6^{(2)} - 3c_{15}^{(2)} = \lambda(z_0 - z_3),\\
&2c_6^{(2)} + c_1^{(2)} - 3c_5^{(2)} = \lambda(z_0 - z_3),\\
&2c_{11}^{(2)} + c_{15}^{(2)} - 3c_{18}^{(2)} = \lambda/3(z_5 - z_4) + 2\lambda/3(z_0 - z_3),\\
&2c_{15}^{(2)} + c_5^{(2)} - 3c_{16}^{(2)} = \lambda(z_0 - z_3),\\
&2c_{18}^{(2)} + c_{16}^{(2)} - 3c_{19}^{(2)} = \lambda/9(z_5 - z_4) + 8\lambda/9(z_0 - z_3),
\end{aligned}
$$

in the direction $u_4 - u_3$, and

$$
\begin{aligned}
&c_3^{(2)} - c_{10}^{(2)} = \lambda(z_5 - z_0),\\
&c_{10}^{(2)} - c_6^{(2)} = \lambda(z_4 - z_3),\\
&c_6^{(2)} - c_1^{(2)} = \lambda(z_0 - z_2),\\
&c_{11}^{(2)} - c_{15}^{(2)} = \lambda/3(z_5 - z_0) + 2\lambda/3(z_4 - z_3),\\
&c_{15}^{(2)} - c_5^{(2)} = \lambda/3(z_0 - z_2) + 2\lambda/3(z_4 - z_3),\\
&c_{18}^{(2)} - c_{16}^{(2)} = \lambda/9(z_5 - z_0) + \lambda/9(z_0 - z_2) + 7\lambda/9(z_4 - z_3),
\end{aligned}
$$

in the direction $u_4 - u_2$. Each set of expressions supports our claim that S preserves monotonicity of L.

Finally we consider similar conditions for the macro-triangle $\langle u_2, u_4, u_6\rangle$, specifically its micro-triangle $\langle u_2, u_4, v_0\rangle$. For the direction $u_4 - u_6$ we get

$$
\begin{aligned}
&c_1^{(4)} + 2c_4^{(4)} - 3c_5^{(4)} = \lambda(z_3 - z_2),\\
&c_4^{(4)} + 2c_9^{(4)} - 3c_{13}^{(4)} = \lambda(z_4 - z_0),\\
&c_9^{(4)} + 2c_2^{(4)} - 3c_8^{(4)} = \lambda(z_4 - z_0),\\
&c_5^{(4)} + 2c_{13}^{(4)} - 3c_{16}^{(4)} = \lambda/3(z_3 - z_2) + \lambda/3(z_4 - z_0) + \lambda/3(z_0 - z_1),\\
&c_{13}^{(4)} + 2c_8^{(4)} - 3c_{17}^{(4)} = \lambda/3(z_5 - z_6) + 2\lambda/3(z_4 - z_0),\\
&c_{16}^{(4)} + 2c_{17}^{(4)} - 3c_{19}^{(4)} = \lambda/9(z_3 - z_2) + 2\lambda/9(z_5 - z_6) + 3\lambda/9(z_4 - z_0) +\\
&+ 3\lambda/9(z_0 - z_1).
\end{aligned}
$$

For the direction $u_4 - u_2$ we get

$$
\begin{aligned}
&-c_1^{(4)} + c_4^{(4)} = \lambda(z_0 - z_2),\\
&-c_4^{(4)} + c_9^{(4)} = \lambda(z_4 - z_3),\\
&-c_9^{(4)} + c_2^{(4)} = \lambda(z_5 - z_0),\\
&-c_5^{(4)} + c_{13}^{(4)} = \lambda/3(z_4 - z_3) + 2\lambda/3(z_0 - z_2),\\
&-c_{13}^{(4)} + c_8^{(4)} = \lambda/3(z_4 - z_3) + 2\lambda/3(z_5 - z_0),\\
&-c_{16}^{(4)} + c_{17}^{(4)} = \lambda/9(z_6 - z_1) + 2\lambda/9(z_4 - z_3) + 3\lambda(z_5 - z_0) + 3\lambda(z_0 - z_2),
\end{aligned}
$$

and for the direction $u_6 - u_2$ we get

$$
\begin{aligned}
&-2c_1^{(4)} - c_4^{(4)} + 3c_5^{(4)} = \lambda(z_0 - z_3),\\
&-2c_4^{(4)} - c_9^{(4)} + 3c_{13}^{(4)} = \lambda(z_0 - z_3),\\
&-2c_9^{(4)} - c_2^{(4)} + 3c_8^{(4)} = \lambda(z_5 - z_4),\\
&-2c_5^{(4)} - c_{13}^{(4)} + 3c_{16}^{(4)} = \lambda/3(z_1 - z_2) + 2\lambda/3(z_0 - z_3),\\
&-2c_{13}^{(4)} - c_8^{(4)} + 3c_{17}^{(4)} = \lambda/3(z_5 - z_4) + \lambda/3(z_6 - z_0) + \lambda/3(z_0 - z_3),\\
&-2c_{16}^{(4)} - c_{17}^{(4)} + 3c_{19}^{(4)} = \lambda/9(z_5 - z_4) + 2\lambda/9(z_1 - z_5) + 3\lambda/9(z_6 - z_0) +\\
&+ 3\lambda/9(z_0 - z_3). \qquad \square
\end{aligned}
$$

4.3. Positivity

According to the equation (3), if on a triangle $\tau^{(i)} = \langle v_1, v_2, v_3\rangle$ the data values z_i, z_2, z_3 are positive, the values $z_j^{(i)}$, $j = 1, 2, 3$ are positive as well. Respectively the spline S is positive on $\tilde{\tau}^{(i)}$ by Theorem 3.3 in Lai and Schumaker (2007), since its coefficients, defined by (5), are positive.

Suppose $L(v)$ is positive on two neighboring triangles $\tau^{(i)}$ and $\tau^{(j)}$. Following the notation used in Sections 2, 3, and 5, it means that the data values z_k, $k = 1, \ldots, 4$ are positive. Respectively, $z_k^{(i)}$ and $z_k^{(j)}$, $k = 1, 2, 3$ are positive as well. By formulas (7)–(10), (12), (13) it is clear that the coefficients $c_k^{(4)}$, $k \in \{1, \ldots, 4, 7, \ldots, 10\}$ are positive. Note that

$$
\begin{aligned}
c_{12} &= 2\lambda z_2 + (1 - 2\lambda)z_3,\\
c_5 &= (1 - 2\lambda)z_2 + 2\lambda z_3
\end{aligned}
$$

are positive and thus so are c_{13}, c_{14} and c_{15}. Similarly, since c_6 and c_{11} can be shown to be positive, so are c_{17}, c_{18}, c_{19}. Now, as long as we can show that c_{16} and c_{20} are positive, the rest will follow. Simplifying c_{16} we get

$$
\frac{(5 - 33\lambda + 45\lambda^2)z_2 + (1 + 3\lambda - 36\lambda^2)z_3 + 3(1 - 3\lambda)\lambda z_4}{3(2 - 9\lambda)}
$$

where each of the quadratic polynomials – coefficients of z_2, z_3 and z_4 – are strictly positive for $0 < \lambda < 1/6$. The result is similar for c_{20}. We thus conclude that

Theorem 9. *If $L(v)$ is positive on two neighboring triangles $\tau^{(i)}$ and $\tau^{(j)}$, then the spline defined on the quadrangle $\tilde{q}^{(i,j)}$ along the edge $e^{(i,j)}$ common to $\tau^{(i)}$ and $\tau^{(j)}$ is positive as well.*

The results are even more straight forward for the coefficients of the spline on 12T macro-elements.

Theorem 10. *If z_i, $i = 0, \ldots 6$ of $\cup_{i=1}^{6}\tau^{(i)}$ are positive, the spline is positive on all t_i, $i = 1, \ldots, 4$.*

Proof. Follow the formulas (15)–(23). $\square$

Clearly, all the shape-preservation properties proved for a triangle t_2 above hold for the macro-elements along the boundary as well. Note also that having S to interpolate L and its derivatives at the chosen locations implies that

$$
\lim_{\lambda \to 0} S = L,
$$

and that completes our results on shape-preserving approximation of L on Δ.

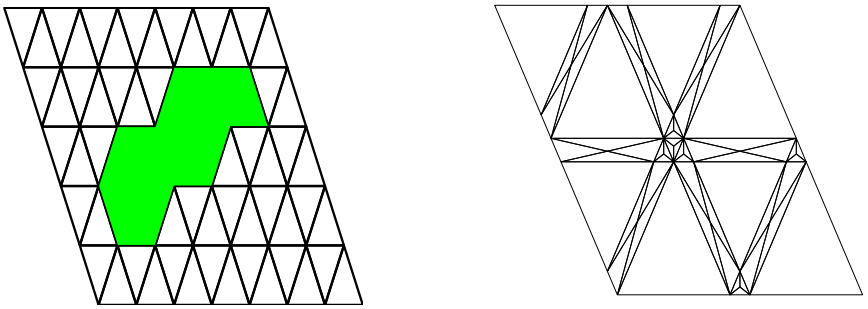

Fig. 8. Left: Type I uniform triangulation. Outlined portion corresponds to a region of "flatness" in Example 1. Right: A portion of the refined triangulation on the left with $\lambda = 0.1$.

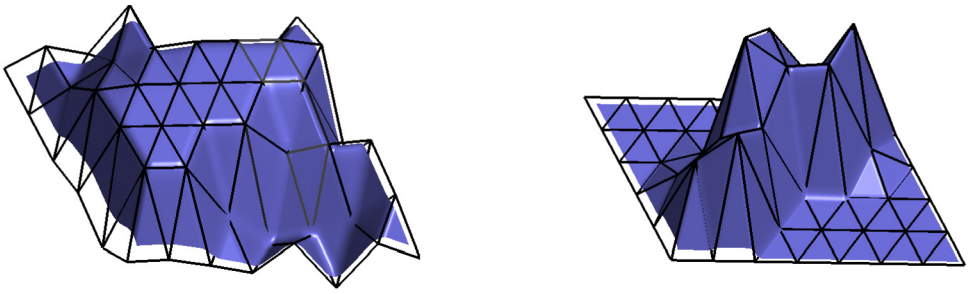

Fig. 9. Left: Piece-wise linear interpolant is presented by a triangular mesh. Spline surface as seen through the mesh preserves its shape. Right: Piece-wise linear interpolant and spline surface of Example 2.

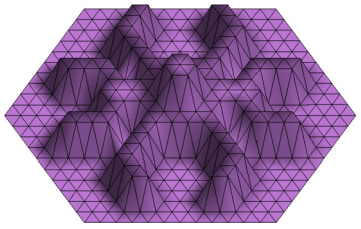

Fig. 10. Piece-wise linear interpolant, Example 3.

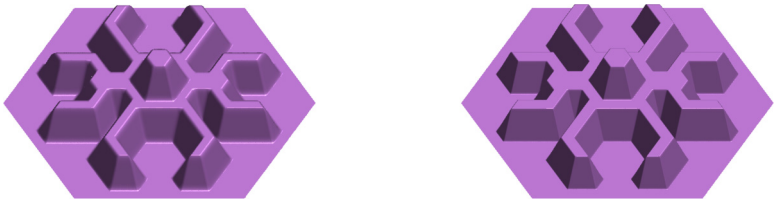

Fig. 11. Approximating splines with different tension parameter values in Example 3.

5. Numerical experiments

In this section we compute several spline surfaces to demonstrate their shape-preserving properties.

Example 1. We begin with a type I uniform triangulation on a 8 by 6 grid of vertices. A z-value at some of the vertices is a random number between 0 and 1, for the rest of the vertices $z = 1$. Fig. 8, left, shows the triangulation and a region outlined by the vertices at which $z = 1$. Fig. 9, left, shows the piece-wise linear and the corresponding shape-preserving smooth cubic spline.

Example 2. On the same grid, z-values are random numbers between 0 and 1 at the vertices of the shaded region of Fig. 8, left. Outside the region the values are $z = 0$. Fig. 9, right, shows the piece-wise linear interpolant and the corresponding spline. In both examples we used $\lambda = 0.1$.

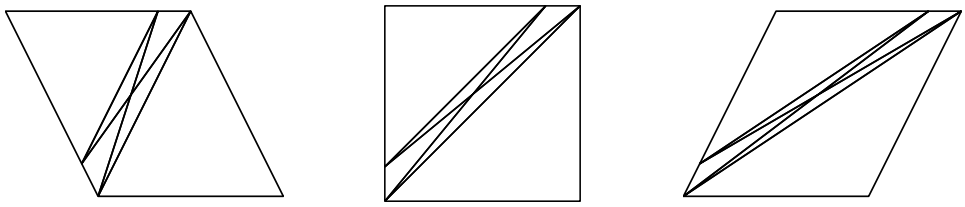

Fig. 12. Triangulations in Example 4.

Table 1
Numerical results for Example 4.

λ	$\|f - s^1_\lambda\|_\infty$	$\|f - s^2_\lambda\|_\infty$	$\|f - s^3_\lambda\|_\infty$
1e−1	7.7716e−16	1.1102e−15	1.3323e−15
1e−2	1.1102e−15	6.6613e−15	2.5535e−14
1e−3	4.8628e−14	6.7724e−14	1.3078e−13
1e−4	4.5519e−14	4.6363e−13	1.0283e−12
1e−5	2.3652e−12	1.0468e−11	1.4482e−11
1e−6	3.8362e−11	1.2986e−10	3.1365e−10

Example 3. In this example we create two shape-preserving splines, each corresponding to a different value of λ. The linear piece-wise interpolant for the data is shown in Fig. 10. The spline, Fig. 11, left, is computed with $\lambda = 0.16$, the figure on the right is for the $\lambda = 0.05$. As expected, smaller values of λ result in spline surfaces with sharper outlined edges.

Example 4. A typical block of $\tilde{\Delta}$, $\lambda = 0.1$, is pictured in Fig. 8, right. It is well known that thin angles cause numerical error, and some of the angles of $\tilde{\Delta}$ are quite small. In this last example we present numerical results investigating the influence of λ on the numerical error in the approximation of $f = x + y$ by a spline over a quadrangle in $\tilde{\Delta}$.

In each of the three cases below we start with just two triangles in Δ. The new partition $\tilde{\Delta}$ consists of two regular triangles and a single quadrangle along the interior edge of Δ. The three triangulations, which vary by the sizes of angles in the initial triangulations, are pictured in Fig. 12, where $\lambda = 0.1$ for all three figures. Let q denote the quadrangle in $\tilde{\Delta}$. We compute a cubic C^1 spline s^i_λ, $i = 1, 2, 3$ on q interpolating the values of a function f and its gradients at the vertices of q. Additionally we interpolate directional derivatives of f at midpoints of the outer edges of q in the directions normal to the respective edges. The remaining spline coefficients are computed to ensure C^1 smoothness across the interior edges of q (see section 6.5 in Lai and Schumaker, 2007 for details). As we vary λ we record the absolute error in the approximation of f by the spline s^i_λ with respect to the infinity norm taken over about 3000 locations in q. Each spline interpolant is expected to reproduce f, and thus the errors recorded in Table 1 are due to the decreasing angles.

In the original triangulation Δ corresponding to Fig. 12, left, the smallest angle is about 53°. The errors for the splines s^1_λ are recorded in the second column of Table 1. In the third column we record similar results for s^2_λ-splines are computed over quadrangles as in $\tilde{\Delta}$ Fig. 12, center, the smallest angle in Δ is 45°. Finally, for the third triangulation the smallest angle is approximately 30°, and the results are recorded in column 4 of the table. Examining results down the table, as λ decreases towards zero, each time by a factor of 10, we loose approximately 1 digit in accuracy. Additionally the smallest angle of the original triangulation decreases as we follow results in the table from left to right, while the error generally increases.

As expected (see equations (2)) the approximation on quadrangles involved in $\tilde{\Delta}$ suffers from small values of λ, as well as from small angles in the initial triangulation. Considering that larger λ's lead to more visually pleasing solutions, in practice we would not anticipate λ's much smaller than 0.1, which would reduce the negative effect of λ on the error. The rest would depend on the initial triangulation Δ.

6. Conclusions

We have shown how to construct a triangulation $\tilde{\Delta}$ that allows us to define a smooth cubic spline interpolating values and gradients of a piece-wise linear function at certain locations. The triangulation and the values to be interpolated are chosen to produce a solution that follows local changes in the behavior of the piece-wise linear function. The spline preserves monotonicity, convexity and positivity of the piece-wise linear function without overshooting. In fact, around each vertex of the initial triangulation, along certain directions the spline is variation diminishing. The scheme uses local data information, and simple explicit formulas for the coefficients of the spline are included.

Numerical examples illustrate shape-preserving behavior of the spline and highlight visual differences induced by the choice of the parameter λ. Last example investigates the influence of λ on angles in quadrangles of $\tilde{\Delta}$ and the resulting loss of accuracy.

Visually examining the solutions we outline several directions in which the results may be improved or modified. Since larger values of λ lead to more rounded looking surfaces, it is interesting to see if the method can be redefined and shape-preserving properties still hold for $\lambda = 1/6$. Additionally it might be possible to improve the solution by adjusting slopes and values interpolated by splines, possibly removing or relaxing the condition that $S \equiv L$ on some of the sub-triangles. Extra degrees of freedom may be introduced by splitting the triangles where the spline is currently flat and using these degrees of freedom to minimize flat areas. It would be interesting to see if similar spline spaces can be defined for higher degrees and smoothness, and whether an additional control over the final look of a shape-preserving surface can be gained from a greater dimension of a spline space.

References

Carlson, R.E., Fritsch, F.N., 1985. Monotone piecewise bicubic interpolation. SIAM J. Numer. Anal. 22, 386–400.

Carlson, R.E., Fritsch, F.N., 1989. An algorithm for monotone piecewise bicubic interpolation. SIAM J. Numer. Anal. 26, 230–238.

Carnicer, J.M., Goodman, T.N., Peña, J.M., 2009. Convexity preserving scattered data interpolation using Powell–Sabin elements. Comput. Aided Geom. Des. 26 (7), 779–796.

Chui, C.K., Diamond, H., Raphael, L., 1989. Shape-preserving quasi-interpolation and interpolation by box spline surfaces. J. Comput. Appl. Math. 25, 169–198.

Costantini, P., Fontanella, F., 1990. Shape-preserving bivariate interpolation. SIAM J. Numer. Anal. 27 (2), 488–506.

Costantini, P., Manni, C., 1991. A local scheme for bivariate co-monotone interpolation. Comput. Aided Geom. Des. 8, 371–391.

Costantini, P., Manni, C., 1999. A local shape-preserving interpolation scheme for scattered data. Comput. Aided Geom. Des. 16, 385–405.

Gilsinn, D.E., Lavery, J.E., 2002. Shape preserving, multiscale fitting of bivariate data by cubic l_1 smoothing splines. In: Chui, J.S.C.K., Schumaker, L.L. (Eds.), Approximation Theory X: Wavelets, Splines, and Applications. Vanderbilt University Press, Nashville, TN, pp. 283–293.

Hussain, M.Z., Sarfraz, M., Shakeel, A., 2011. Shape preserving surfaces for the visualization of positive and convex data using rational bi-quadratic splines. Int. J. Comput. Appl. 27 (10), 12–20.

Kouibia, A., Pasadas, M., 2003. Variational bivariate interpolating splines with positivity constraints. Appl. Numer. Math. 44 (4), 507–526.

Kuijt, F., Damme, R.V., 2001. A linear approach to shape preserving spline approximation. Adv. Comput. Math. 14 (1), 25–48.

Lai, M.J., 2000. Convex preserving scattered data interpolation using bivariate c^1 cubic splines. J. Comput. Appl. Math. 119 (1), 249–258.

Lai, M.J., Meile, C., 2015. Scattered data interpolation with nonnegative preservation using bivariate splines and its application. Comput. Aided Geom. Des. 34, 37–49.

Lai, M.J., Schumaker, L.L., 2007. Spline Functions on Triangulations. Encyclopedia of Mathematics and Its Applications, vol. 110. Cambridge University Press.

Lai, M.J., Wenston, P., 2004. L1 spline methods for scattered data interpolation and approximation. Adv. Comput. Math. 21, 293–315.

Lavery, J.E., 2001. Shape preserving, multiscale interpolation by bi- and multivariate cubic l_1 splines. Comput. Aided Geom. Des. 18, 321–343.

Leung, N.K., Renka, R.J., 1999. c^1 convexity-preserving interpolation of scattered data. SIAM J. Sci. Comput. 20, 1732–1752.

Li, A., 1999. Convexity preserving interpolation. Comput. Aided Geom. Des. 16 (2), 127–147.

Manni, C., 2001. Local tension methods for bivariate scattered data interpolation. In: Lyche, T., Schumaker, L.L. (Eds.), Mathematical Methods for Curves and Surfaces. Vanderbilt University Press, Nashville, TN, pp. 293–314.

Rayevskaya, V., Schumaker, L.L., 2005. Multi-sided macro-element spaces based on Clough–Tocher triangle splits with applications to hole filling. Comput. Aided Geom. Des. 22 (1), 57–79.

Schmidt, J.W., 1999. Range restricted interpolation by cubic c^1-splines on Clough–Tocher splits. Math. Res. 107, 253–268.

Schmidt, J.W., Hess, W., 1993. S-convex, monotone, and positive interpolation with rational bicubic splines of c2-continuity. BIT Numer. Math. 33 (3), 496–511.

Schumaker, L.L., Han, L., 1997. Fitting monotone surfaces to scattered data using c^1 piecewise cubics. SIAM J. Numer. Anal. 34, 569–585.

Schumaker, L.L., Speleers, H., 2010. Nonnegativity preserving macro-element interpolation of scattered data. Comput. Aided Geom. Des. 27 (3), 245–261.

Schumaker, L.L., Speleers, H., 2011. Convexity preserving splines over triangulations. Comput. Aided Geom. Des. 28 (4), 270–284.

Utreras, F., 1985. Positive thin plate splines. Approx. Theory Appl. 1 (3), 77–108.

Willemans, K., Dierckx, P., 1994. Surface fitting using convex Powell–Sabin splines. J. Comput. Appl. Math. 56 (3), 263–282.

Willemans, K., Dierckx, P., 1995. Nonnegative surface fitting with Powell–Sabin splines. Numer. Algorithms 9 (2), 263–276.

Witzgall, C., Gilsinn, D.E., McClain, M.A., 2006. An examination of new paradigms for spline approximations. J. Res. Natl. Inst. Stand. Technol. 111 (2), 57.